Chemical Science

Accepted Manuscript

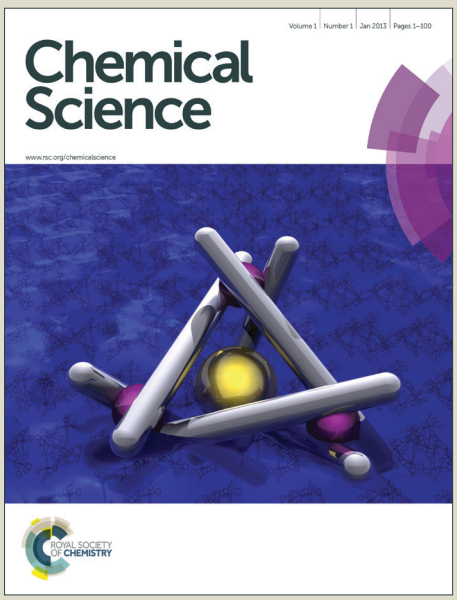

ROYAL SOCIETY OF CHEMISTRY

www.rsc.org/chemicalscience

Unexpected effect of catalyst concentration on photochemical CO_2 reduction by *trans*(Cl)-$Ru(bpy)(CO)_2Cl_2$: new mechanistic insight into the $CO/HCOO^-$ selectivity

Yusuke Kuramochi,[†] Jun Itabashi,[†] Kyohei Fukaya,[†] Akito Enomoto,[†] Makoto Yoshida,[†] and Hitoshi Ishida[†, ‡]*

[†]Department of Chemistry, Graduate School of Science, Kitasato University, 1-15-1 Kitasato, Minami-ku, Sagamihara, Kanagawa 252-0373, Japan.

[‡] Precursory Research for Embryonic Science (PRESTO), Japan Science and Technology Agency (JST), 4-1-8 Honcho, Kawaguchi, Saitama, 332-0012, Japan

Abstract

Photochemical CO_2 reduction catalysed by *trans*(Cl)-Ru(bpy)$(CO)_2Cl_2$ (bpy = 2,2'-bipyridine) efficiently produces carbon monoxide (CO) and formate ($HCOO^-$) in *N,N*-dimethylacetamide (DMA)/water containing $[Ru(bpy)_3]^{2+}$ as a photosensitizer and 1-benzyl-1,4-dihydronicotinamide (BNAH) as an electron donor. We have unexpectedly found catalyst concentration dependence on the product ratio ($CO/HCOO^-$) in the photochemical CO_2 reduction: the ratio of $CO/HCOO^-$ decreases by increasing the catalyst concentration. The result has led us to propose a new mechanism in which $HCOO^-$ selectively produces by formation of the Ru(I)-Ru(I) dimer as the catalyst intermediate. The reaction mechanism predicts that the Ru-Ru bond dissociates in the reaction of the dimer with CO_2 and that the insufficient electron supply to the catalyst results in the dominant formation of $HCOO^-$. The proposed mechanism is supported by the results that the time-course profiles of CO and $HCOO^-$ in the photochemical CO_2 reduction catalysed by $[Ru(bpy)(CO)_2Cl]_2$ (0.05 mM) are very similar to those by *trans*(Cl)-Ru(bpy)$(CO)_2Cl_2$ (0.10 mM) and that the $HCOO^-$ formation becomes dominant at low-intensity light. The kinetic analyses based on the proposed mechanism could exquisitely reproduce the unusual catalyst concentration effect on the products ratio. The catalyst concentration effect observed in the photochemical CO_2 reduction using $[Ru(4dmbpy)_3]^{2+}$ (4dmbpy = 4,4'-dimethyl-2,2'-bipyridine) instead of $[Ru(bpy)_3]^{2+}$ as the photosensitizer is also explained with the kinetic analyses, reflecting the smaller quenching rate constant of the excited $[Ru(4dmbpy)_3]^{2+}$ by BNAH than that of the excited $[Ru(bpy)_3]^{2+}$. We have further synthesized *trans*(Cl)-Ru(6Mes-bpy)$(CO)_2Cl_2$ (6Mes-bpy = 6,6'-dimesityl-2,2'-bipyridine), which bears the bulky substituents at 6,6'-positions in the 2,2'-bipyridyl ligand, so that the ruthenium complex cannot form the dimer

due to the steric hinderance. We have found that the ruthenium complex selectively produces CO, which strongly supports the catalytic mechanism proposed in this work.

Introduction

Photocatalytic CO_2 reduction represents a major concern in relation to construction of artificial photosynthetic systems and solar fuels, which are relevant to the solution of the fossil fuel shortage and the global warming problems.[1-4] Until now, a lot of metal complexes have been researched for the CO_2 reduction catalyses.[5-15] As the metal complexes for the catalysts, manganese mono(bipyridyl) tricarbonyl,[16-18] cobalt and iron porphyrin,[19-21] cobalt tris(bipyridyl)[22] and macrocycle,[23,24] nickel cyclam,[25,26,27] molybdenum and tungsten mono(bipyridyl) tetracarbonyl,[28] rhodium bis(bipyridyl),[29-30] palladium phosphine,[31-33] rhenium mono(bipyridyl) tricarbonyl,[34-42] osmium mono(bipyridyl) dicarbonyl,[43,44] iridium poly(pyridyl) and dihydride pincer,[45,46] ruthenium mono(bipyridyl) and bis(bipyridyl) dicarbonyl complexes[47-70] have been researched. Most of them yield CO and/or formate as the two-electron reduction product of CO_2. In the metal complex catalysts, the ruthenium complexes (e.g., $[Ru(bpy)_2(CO)_2]^{2+}$) have actively been studied for the $CO/HCOO^-$ selectivity. In the catalyses, the product selectivity depends on the reaction conditions: the acidic condition enhances the CO production while the basic condition causes the formate production.[51-56,69] The photochemical reductions have mostly accompanied with the formate production[47-49,51-53,57-62,70] while the electrochemical reductions have achieved the selective formation of CO.[55,63-69] The reaction mechanisms of the Ru(II) complexes have been proposed as shown in Scheme 1.[50-56,69] The widely accepted mechanism for the CO production is as follows: 1) the Ru(II) complex accepts one electron to release CO, 2) the one-electron-reduced complex accepts another electron, and 3) the two-electron-reduced complex undergoes an electrophilic attack by CO_2 along with protonation and dehydration to reproduce the starting Ru(II) complex. For the formate production, two mechanisms have been proposed so far. Tanaka and co-authors have proposed

the mechanism in which the equilibrium between $[Ru\text{-}C(O)OH]^{(n+1)+}$ and $[Ru\text{-}CO]^{(n+2)+}$ governs the product selectivity of $CO/HCOO^-$: the two-electron reduction of $[Ru\text{-}C(O)OH]^{(n+1)+}$ causes the formate production.[51-56,69] This mechanism can elucidate it well that formate mainly produces under basic conditions where the equilibrium shifts to the hydroxycarbonyl complex. However, it is not fully accepted because the reaction requires the specific proton attack on the carbon atom of the hydroxycarbonyl group. Meyer *et al.* have proposed that formate generates *via* insertion of CO_2 into the Ru-H bond in $[Ru\text{-}H]^{n+}$.[50] The mechanism *via* the hydride complex is based on the experimental results that $[Ru(bpy)_2(CO)H]^0$ reacts with CO_2 to yield $[Ru(bpy)_2(CO)(OC(O)H)]^0$, and generally accepted as a formate production in the organometallic chemistry. However, this mechanism does not successfully elucidate why formate selectively produces under the less protic conditions and why dihydrogen originating from the hydride intermediate does scarcely evolve with formate but CO. Even today with more than 20 years having passed since these mechanisms were proposed, consensus on the reaction mechanism for the formate production has not yet been reached.

Scheme 1. Combined Mechanisms[48] Proposed by Tanaka *et al.*[69] and Meyer *et al.*[50]

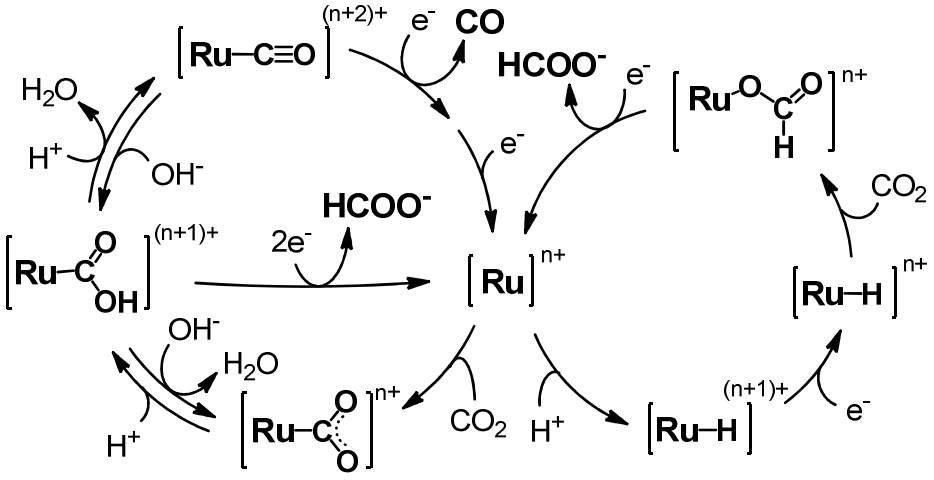

Recently, polymeric ruthenium mono(bipyridyl) dicarbonyl complexes (e.g., $[Ru(L)(CO)_2]_n$ (L = bipyridyl derivatives)) have been utilized as the reduction catalysts in the artificial photosynthetic systems using semiconductors, which can utilize water as electron donor.[60] The system consists of TiO_2 and InP modified with the ruthenium polymer, and the photo-irradiation to the system induces the electron transfers from the semiconductors to the ruthenium polymer which catalyses the CO_2 reduction using the electrons to afford formate in 10 mM $NaHCO_3$ aqueous solution with CO_2 bubbling. The polymeric ruthenium mono(bipyridyl) dicarbonyl complexes have been reported as the catalysts in the electrochemical CO_2 reduction by Deronzier and Ziessel *et al.*[63-65,67,68] The selectivity for the CO vs. formate production depends essentially on the substituents which are introduced at 4,4'position of the bipyridyl ligand in aqueous solution.[64] The ruthenium mono(bipyridyl) dicarbonyl polymers and the derivatives with electron-donating substituents give mainly CO as reduction product at pH 6. The pH values in the solution and the electrolytes (e.g., $NaSO_4$ vs. $LiClO_4$) used for the electrolyses moderately affect the selectivity. To the contrary, the polymer complexes with electron-withdrawing substituents quantitatively yield $HCOO^-$. This difference is elucidated as the

electronic structures of the catalyst intermediates (the hydroxycarbonyl or formato complexes) formed during the electrocatalytic process. The similar tendency has been reported for the electrocatalyses by the derivatives of $[Ru(bpy)_2(CO)_2]^{2+}$.[69] Thus, the results from literatures indicate that the reaction mechanisms and the product selectivity strongly depend on the reaction conditions. However, to the best of our knowledge, there is no report on the catalyst concentration effects on the product selectivity in CO_2 reduction.

Scheme 2. Formation of Polymeric Ruthenium Complex from *trans*(Cl)-Ru(bpy)$(CO)_2Cl_2$

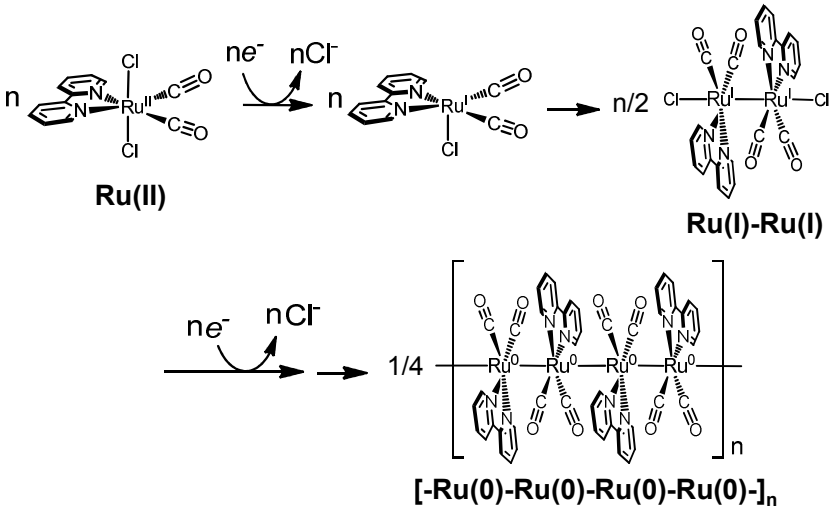

The polymeric ruthenium mono(bipyridyl) dicarbonyl complexes are obtained by electrochemical reductions of mono(bipyridyl) dicarbonyl dichloride complexes.[63-65,67,68,71,72] as well as ruthenium bis(bipyridyl) dicarbonyl complexes.[66] For instance, the formation process of $[Ru(bpy)(CO)_2]_n$ is shown in Scheme 2. The electrochemical reduction of Ru(bpy)$(CO)_2Cl_2$ initially dissociates the chloride ion to form a dimer, $[Ru(bpy)(CO)_2Cl]_2$, which has already been

elucidated by Haukka *et al.* with the X-ray crystallographic analysis.[73] Further reduction of the ruthenium dimer causes dissociation of the chloride ions to give $[Ru(bpy)(CO)_2]_n$. The monomeric ruthenium complex, $Ru(bpy)(CO)_2Cl_2$, also shows the catalytic activity for the electrochemical CO_2 reduction,[63,65,67,69] but the complex tends to form an adherent film of the polymer on the electrode during the electrochemical CO_2 reduction, making it difficult to investigate the catalytic properties of the monomeric complex in detail. The photochemical CO_2 reduction catalysed by $Ru(bpy)(CO)_2Cl_2$ have been reported in the presence of $[Ru(bpy)_3]^{2+}$ as the photosensitizer and triethanolamine (TEOA) as the electron donor,[70] in which the reaction starts when $[Ru(bpy)_3]^{2+}$ absorbs the visible light to induce the electron transfer relay from TEOA to the catalyst. However, the system also causes the black precipitation of the polymeric complex during the catalytic reaction and it probably inhibits light absorption and/or electron transfer from the photosensitizer.

We have very recently reported the photochemical CO_2 reduction catalysed by $[Ru(bpy)_2(CO)_2]^{2+}$ in *N,N*-dimethylacetamide (DMA)/water containing $[Ru(bpy)_3]^{2+}$ and 1-benzyl-1,4-dihydronicotinamide (BNAH).[47] DMA is used as the alternative solvent of *N,N*-dimethylformamide (DMF), which is the most frequently used solvent in the photochemical CO_2 reduction but has been indicated to cause contamination of $HCOO^-$ from the hydrolysis.[74] In the DMA/water systems using BNAH as the electron donor, the black precipitates have scarcely formed and the photocatalytic CO_2 reduction has smoothly proceeded. The products are CO and formate, which have been confirmed as the CO_2 reduction products by the ^{13}C NMR experiments. We have further exhibited that the oxidized form of BNAH is the BNA dimers, *e.g.*, 1,1'-dibenzyl-1,1',4,4'-tetrahydro-4,4'-binicotinamide (4,4'-BNA_2),[47,49] indicating that the reduced

species of the photosensitizer ($[Ru(bpy)_3]^+$), which generates by the reductive quenching of the excited $[Ru(bpy)_3]^{2+}$ with BNAH, supplies the electrons to the catalyst.

In this work, we have investigated the photochemical CO_2 reduction catalysed by *trans*(Cl)-Ru(bpy)$(CO)_2Cl_2$ in the DMA/water solution containing $[Ru(bpy)_3]^{2+}$ and BNAH (Figure 1). We have unexpectedly discovered that the concentration of *trans*(Cl)-Ru(bpy)$(CO)_2Cl_2$ affects the product selectivity ($CO/HCOO^-$). The mechanisms reported so far[48,50-56,64,69,70] cannot elucidate the phenomenon. It motivates us to reconsider the reaction mechanism in the photochemical CO_2 reduction. We propose a new reaction mechanism including the Ru(I)-Ru(I) dimer, which catalyses CO_2 reduction to selectively produce formate, because the ratio of the $HCOO^-$ production become dominant on the low-intensity light, in which the Ru-Ru bond tends to form. The photochemical CO_2 reduction catalysed by $[Ru(bpy)(CO)_2Cl]_2$ (0.05 mM) shows the similar time-course profiles for the CO and $HCOO^-$ production to those by *trans*(Cl)-Ru(bpy)$(CO)_2Cl_2$ (0.10 mM), indicating that the immediate dissociation of the dimer occurs to reproduce the monomeric complex during the CO_2 reduction. We have carried out the kinetic analyses based on the new reaction mechanism, and the simulation curve well reproduces the concentration dependence on the product selectivity ($CO/HCOO^-$). In order to further verify the proposed mechanism, we have synthesized *trans*(Cl)-Ru(6Mes-bpy)$(CO)_2Cl_2$ (Figure 1, 6Mes-bpy: 6,6'-dimesityl-2,2'-bipyridine) which cannot form the dimer due to the bulky substituents at 6,6'-positions in 2,2'-bipyridine. The photochemical CO_2 reduction catalysed by *trans*(Cl)-Ru(6Mes-bpy)$(CO)_2Cl_2$ selectively produces CO, strongly supporting our proposed mechanism for the formate production.

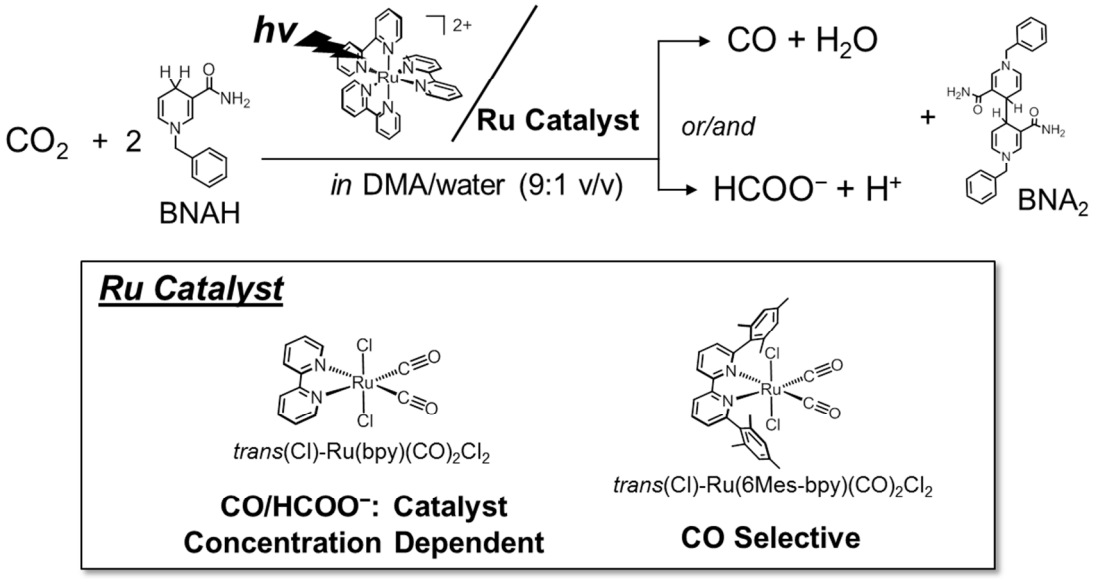

Figure 1. Photochemical CO_2 reduction catalysed by *trans*(Cl)-Ru(bpy)$(CO)_2Cl_2$ or *trans*(Cl)-Ru(6Mes-bpy)$(CO)_2Cl_2$ in the DMA/water solution containing $[Ru(bpy)_3]^{2+}$ and BNAH as the photosensitizer and the electron donor, respectively.

Experimental section

General procedure

$[Ru(bpy)(CO)_2Cl]_2$, $[Ru(CO)_2Cl_2]_n$, *trans*(Cl)-$Ru(bpy)(CO)_2Cl_2$, $[Ru(bpy)_3](PF_6)_2$, $[Ru(4dmbpy)_3](PF_6)_2$ (4dmbpy = 4,4'-dimethyl-2,2'-bipyridine), 6,6'-dimesityl-2,2'-bipyridine (6Mes-bpy), and BNAH were prepared according to the literature.[73,75-78] DMA (Wako, dehydrate) was used as supplied. High-purity water (resistivity: 18.2 MΩ cm) was obtained by an ultrapure water system (RFU424TA, Advantec). Cyclic voltammograms (CVs) and differential pulse voltammograms (DPVs) were obtained by a Bio-Logic VSP Potentiostat using an EC-Lab software. As the electrodes, a BAS glassy-carbon working electrode, a BAS Pt counter electrode, and a BAS RE-7 ($Ag/AgNO_3$ 0.01 M in acetonitrile) reference electrode were used. Absorption spectra in the spectroelectrochemical experiments were obtained on an ALS SEC2000 using an electrochemical cell of 1 mm path length incorporating the three-electrode system.

Synthesis of *trans*(Cl)-$Ru(6Mes\text{-}bpy)(CO)_2Cl_2$

In a 30 mL flask equipped with a reflux condenser were placed $[Ru(CO)_2Cl_2]_n$ (30 mg), 6,6'-dimesityl-2,2'-bipyridine (6Mes-bpy; 51 mg, 0.13 mmol) and ethanol (6 mL) under argon atmosphere, and the solution was refluxed for 18 h. As the reaction proceeded, the starting solution became a white suspension. The precipitation was filtrated and washed with ethanol. The solid was recrystallized from $CHCl_3$-ether to afford a pale yellow crystal (45 mg, 56%): ^1H NMR (400 MHz, $CDCl_3$) δ 8.26 (d, J = 8.0 Hz, 2H), 8.09 (dd. J = 8.0 and 7.6 Hz, 2H), 7.45 (d. J = 7.6 Hz, 2H), 6.97 (s, 4H), 2.33 (s, 6H), 2.16 (s, 12H); FTIR (KBr) ν_{CO} /cm^{-1} 1986, 2051; Anal. Calcd (%) for $C_{30}H_{28}Cl_2N_2O_2Ru$: C, 58.07; H, 4.55; N, 4.51. Found: C, 58.11; H, 4.76; N, 4.65.

Photocatalytic CO_2 reduction

Solutions (5 mL) of the catalyst (*trans*(Cl)-Ru(bpy)$(CO)_2Cl_2$ or *trans*(Cl)-Ru(6Mes-bpy)$(CO)_2Cl_2$), $[Ru(bpy)_3](PF_6)_2$ and BNAH in Ar-saturated DMA/water were placed in quartz tubes (23 mL volume, *i.d.* = 14 mm). The solutions were bubbled through septum caps with CO_2 gas for 20 min, and then were irradiated using a 400 W high-pressure mercury lamp at $\lambda > 400$ nm (Riko Kagaku, L-39 cutoff filter) in a merry-go-round irradiation apparatus (Riko Kagaku, RH400-10W). The reaction temperature was maintained at 298 ± 3 K by using a water bath. The gaseous products (CO and H_2) were analyzed with GC, and formate was also quantified with GC by acidifying formate to formic acid.[47]

Quenching experiments

Emission from the excited state of $[Ru(4dmbpy)_3](PF_6)_2$ in the Ar-saturated DMA/water solution was recorded on a Hitachi F-4500 spectrometer (λ_{ex} = 453 nm) in the absence and the presence of the quencher, BNAH. The Stern-Volmer relationship (eq. 1) was obtained by the plots of the relative emission intensity (I_0/I) versus the concentration of the quencher (Q: BNAH):

$$I_0/I = 1 + K_{SV}[Q] = 1 + k_q\tau[Q] \qquad (1)$$

where I_0 and I represent the intensity at 628 nm in the absence and the presence of the quencher, respectively, and K_{sv}, k_q, τ are the Stern-Volmer constant, the quenching rate constant, and the emission lifetime, respectively.

Light intensity dependence

In square quartz cells (l = 1.0 cm) were placed DMA/water (9:1 v/v, 3 mL) solutions containing Ru catalyst, $[Ru(bpy)_3](PF_6)_2$ and BNAH, and bubbled through septum caps by CO_2 for a least 30 min before measurement. The solutions were irradiated using a 500 W superhigh-pressure

mercury lamp (Ushio, USH-500D) through a Toshiba Y-43 glass filter (λ > 400 nm) with and without neutral-density (ND) filters. The absorption spectral changes of the solutions were measured with a Shimadzu MultiSpec-1500 Spectrometer. The gaseous products (CO and H_2) were analysed with GC, and formate was also quantified with GC by acidifying formate to formic acid.[47]

Results and discussion

Photochemical CO_2 reduction catalysed by *trans*(Cl)-Ru(bpy)$(CO)_2Cl_2$

The photocatalytic CO_2 reductions were carried out in the DMA/water (9:1 v/v) solutions containing *trans*(Cl)-Ru(bpy)$(CO)_2Cl_2$ (the catalyst), $[Ru(bpy)_3]^{2+}$ (the photosensitizer) and BNAH (the electron donor) under the irradiation of visible light (λ >400 nm), where $[Ru(bpy)_3]^{2+}$ was selectively excited and reductively quenched by BNAH to yield the reduced species of the photosensitizer, $[Ru(bpy)_3]^{+}$.[47] The 10 vol.% water content was selected for the reaction solvent because the water ratio gave the highest amount of the reduction products. The water in the reaction solution would play an important role as the transporter of the protons for the CO_2 reduction, but the higher contents of water decrease the quenching efficiencies of BNAH toward $[Ru(bpy)_3]^{2+*}$.[47] The reduction potential of *trans*(Cl)-Ru(bpy)$(CO)_2Cl_2$, which is estimated to be −1.51 V vs. Ag/Ag^+ in DMA/water (9:1 v/v) with the use of the differential pulse voltammetry (Figure S1 in Supporting Information), indicates that the electron transfer can thermodynamically occur from the reduced photosensitizer ($[Ru(bpy)_3]^{2+/+}$: −1.68 V vs. Ag/Ag^+)[47] to *trans*(Cl)-Ru(bpy)$(CO)_2Cl_2$.

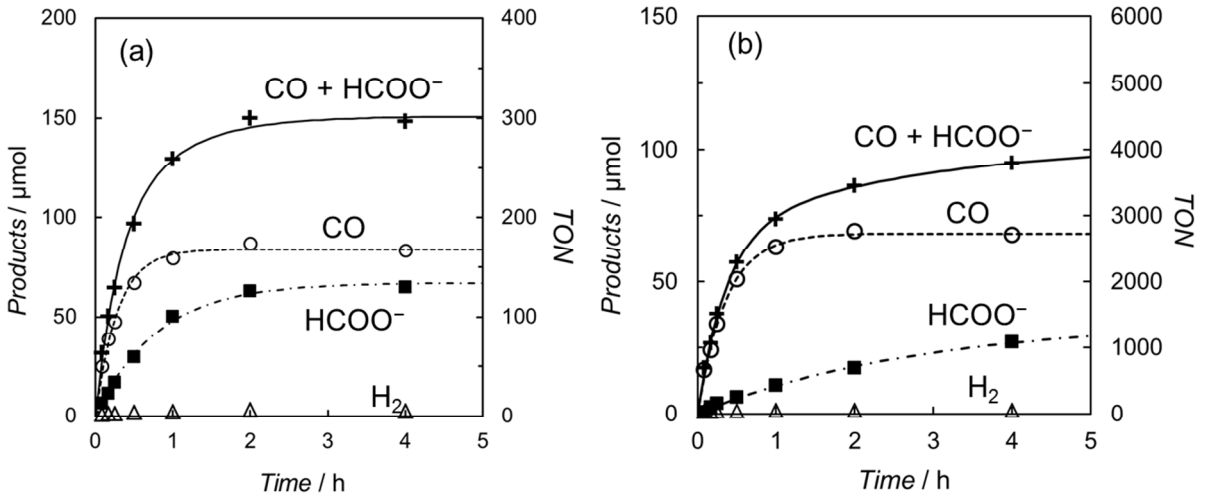

Figure 2. Photo-irradiation time dependence of the products in the CO_2-saturated DMA/water (9:1 v/v) solution containing (a) 0.1 mM and (b) 5.0 μM of *trans*(Cl)-Ru(bpy)$(CO)_2Cl_2$, $[Ru(bpy)_3](PF_6)_2$ (0.50 mM) and BNAH (0.10 M): CO (○), $HCOO^-$ (■), H_2 (Δ) and CO + $HCOO^-$ (+).

Figure 2 shows the time-courses of the products in the photochemical CO_2 reduction in the CO_2-saturated DMA/water (9:1 v/v) solution containing *trans*(Cl)-Ru(bpy)$(CO)_2Cl_2$ ((a) 0.10 mM and (b) 5.0 μM), $[Ru(bpy)_3]^{2+}$ (0.50 mM) and BNAH (0.10 M). The profiles exhibit that CO and formate selectively yield with scarcely accompanying H_2 evolution even in the aqueous solutions, suggesting that the reduced catalyst much favourably reacts with CO_2 than H^+. The turnover number (TON) for the total amount of CO and formate was *ca.* 300 at 0.10 mM of the catalyst after the photo-irradiation for 4 h. When 5.0 μM of *trans*(Cl)-Ru(bpy)$(CO)_2Cl_2$ was used, the TON was dramatically improved to reach *ca.* 4000, because there was no superfluous catalyst at the low concentration. However, the formation of the products stops at longer time. In our

previous work, we reported that the factors are mainly attributable to the decrease of BNAH and the increase of BNA_2.[47] The latter depresses the photochemical CO_2 reduction because BNA_2 reductively quenches the excited state of $[Ru(bpy)_3]^{2+}$ faster than BNAH but the back electron transfer is much more efficient.

It is worth noting that the product ratio of $CO/HCOO^-$ in Figure 2 shows notably higher at 5.0 μM of *trans*(Cl)-$Ru(bpy)(CO)_2Cl_2$ than that at 0.1 mM. For example, the ratio of $CO/HCOO^-$ is approximately 2 at 0.1 mM of the catalyst while *ca.* 7 at 5.0 μM after 30 min of the photo-irradiation. Figure 3 shows concentration dependences of the catalyst on the amounts of CO and formate and the product ratio of $CO/HCOO^-$ after 30 min of the photo-irradiation, which reflects the initial reaction rates of the CO_2 reduction. In Figure 3 bottom, the once raised product ratio of $CO/HCOO^-$ is lowered by increasing the catalyst concentration. The unexpected profile of the product ratio comes from the different behaviour between the initial production rates of CO and formate: the rate of CO formation increases as the catalyst concentration increases by 20−30 μM, and it decreases at more than 30 μM, while the rate of formate production continues to increase as the catalyst concentration increases. In Figure 3 bottom, the raise of the product ratio by increasing of the catalyst concentration from 0 to 5.0 μM would come from contribution of the blank products, which are detected even in the absence of *trans*(Cl)-$Ru(bpy)(CO)_2Cl_2$. It has been known that $[Ru(bpy)_3]^{2+}$ releases the bipyridyl ligand by photo-labilization to provide catalytically active species, resulting in the blank products.[57,70] Amounts of the blank products are 11 and 4 μmol for CO and formate, respectively, and the blank product ratio of $CO/HCOO^-$ is *ca.* 3. Thus, if the blank products caused by $[Ru(bpy)_3]^{2+}$ is excluded, the selectivity of CO would continue to be raised by decreasing the catalyst concentration.

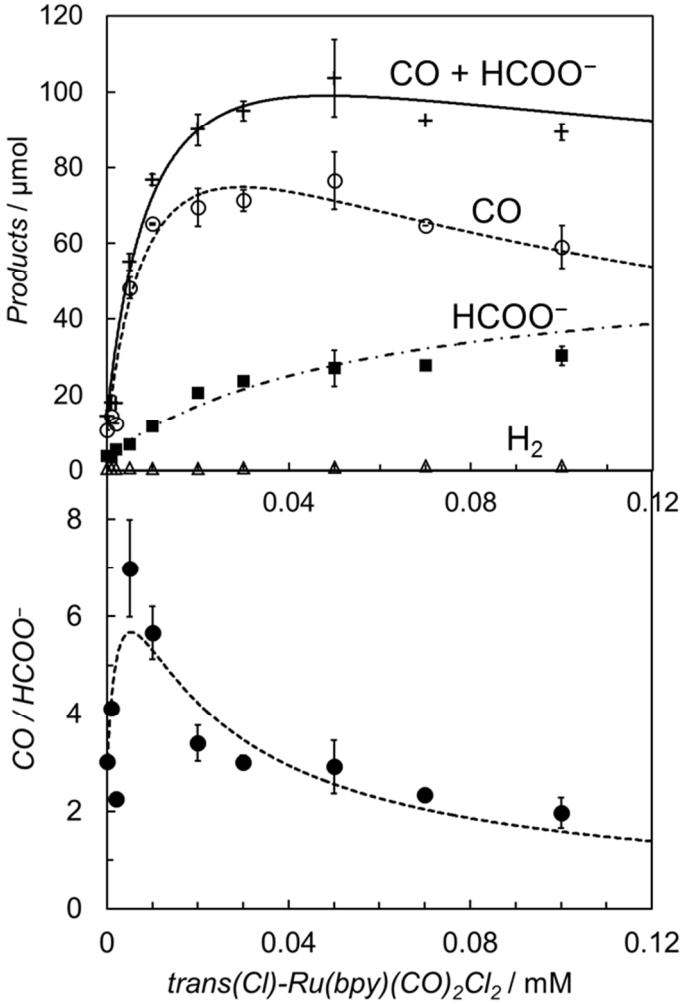

Figure 3. (Top) Plots of the reduction products after 30 min of the photo-irradiation (400 W Hg lamp, λ > 400 nm) versus the concentration of *trans*(Cl)-Ru(bpy)$(CO)_2Cl_2$ in CO_2-saturated DMA/water (9:1 v/v) in the presence of $[Ru(bpy)_3](PF_6)_2$ (0.50 mM), BNAH (0.10 M): CO (○), $HCOO^-$ (■), H_2 (Δ) and CO + $HCOO^-$ (+). (Bottom) Plots of CO/$HCOO^-$ ratio versus the concentration of *trans*(Cl)-Ru(bpy)$(CO)_2Cl_2$. The curves represent the theoretical fittings based on the kinetic analyses (see equations (3) and (5)).

Electronic absorption spectral changes during the photo-irradiation and light intensity dependence of the product selectivity

As shown in Figure 3, the product selectivity of CO/$HCOO^-$ was affected by the catalyst concentration. The behaviour led us to consider that an association of the catalyst occurs during the CO_2 reduction. The photo-irradiation to Ar-saturated DMA/water solution containing *trans*(Cl)-Ru(bpy)$(CO)_2Cl_2$ (0.20 mM), $[Ru(bpy)_3]^{2+}$ and BNAH produced H_2 instead of CO and formate. During the photo-irradiation, the solution colour changed from orange to dark red. The spectral changes of the Ar-saturated reaction solution showed appearance of a characteristic broad peak at 700−800 nm (Figure 4a), indicating that the polymeric ruthenium complex, $[Ru(bpy)(CO)_2]_n$, formed by reduction of *trans*(Cl)-Ru(bpy)$(CO)_2Cl_2$.[49,79,80] On the other hand, the photo-irradiation (400 W high-pressure mercury lamp without the ND filter, $\lambda > 400$ nm) under CO_2 atmosphere showed no colour change of the solution, suggesting that the reduced catalyst was oxidized by coordination with CO_2 to suppress the formation of the polymeric complex. It has been reported that *trans*(Cl)-Ru(bpy)$(CO)_2Cl_2$ is electrochemically reduced to form the polymeric ruthenium complex *via* the Ru(I)-Ru(I) dimer (Scheme 1).[71,72] As the absorption band of the dimer overlaps with that of $[Ru(bpy)_3]^{2+}$ (Figure 4b), the formation of the dimer could not be observed by the absorption spectral change. Thus, if an association of the catalysts relates to the product selectivity of CO/$HCOO^-$ and the absorption spectral change of the reaction solution is not observed during the photo-irradiation, the associated species might be the ruthenium dimeric complex.

Figure 4c and 4d show the spectral changes during the photochemical CO_2 reduction under high- and low-intensity light (500 W superhigh-pressure mercury lamp without and with the ND filters, $\lambda > 400$ nm). The irradiation time is adjusted for the total incident light to be

2.3×10^{-4} einstein. While no spectral change is observed in Figure 4c, the polymeric absorption at 700−800 nm appears in Figure 4d. This indicates that the Ru-Ru bond tends to form under the lower-intensity light.

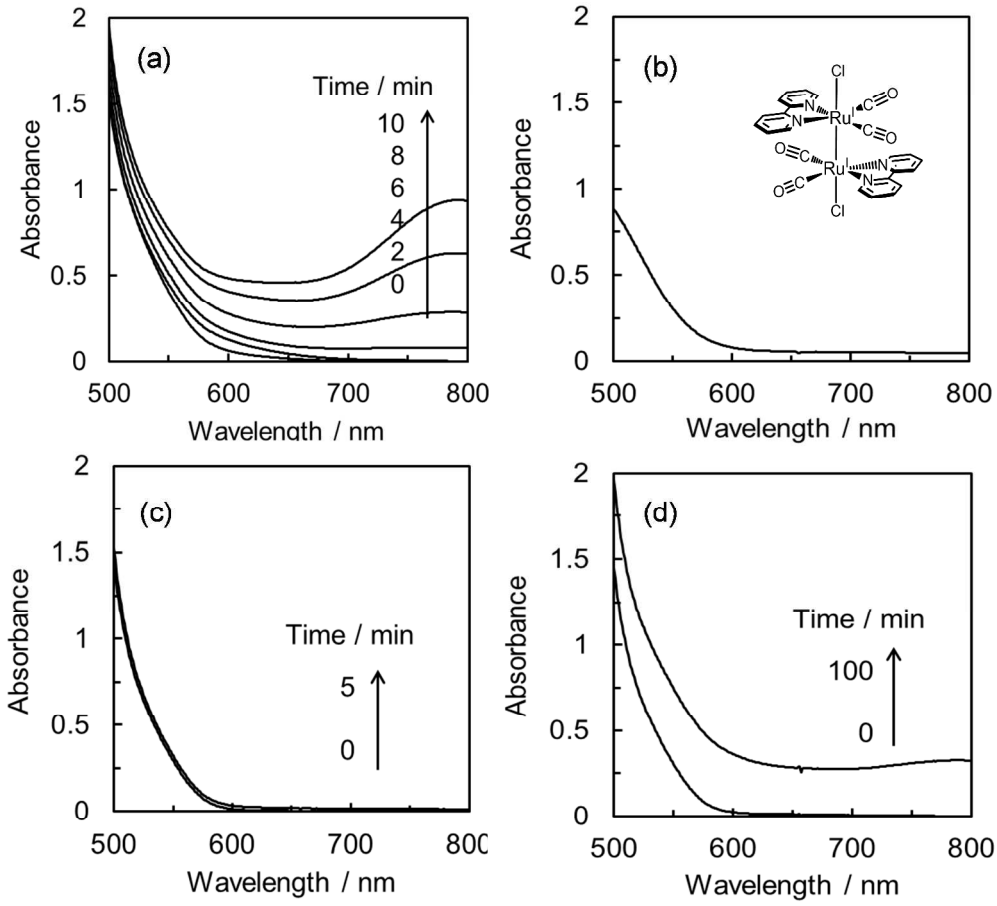

Figure 4. (a) Absorption spectral changes of Ar-saturated DMA/water (9:1 v/v) solution containing *trans*(Cl)-Ru(bpy)$(CO)_2Cl_2$ (0.20 mM), $[Ru(bpy)_3](PF_6)_2$ (0.50 mM) and BNAH (0.10 M) during photo-irradiation of $\lambda > 400$ nm light with intensity of 7.5×10^{-7} einstein s^{-1}. (b) Absorption spectrum of $[Ru(bpy)(CO)_2Cl]_2$ (0.40 mM) in DMA/water (9:1 v/v). (c) Absorption spectral changes of CO_2-saturated DMA/water (9:1 v/v) solutions containing *trans*(Cl)-Ru(bpy)$(CO)_2Cl_2$ (0.10 mM), $[Ru(bpy)_3](PF_6)_2$ (0.50 mM) and BNAH (0.10 M) by photo-irradiation of $\lambda > 400$ nm light of 7.5×10^{-7} einstein s^{-1} and (d) 3.8×10^{-8} einstein s^{-1} (total incident light: 2.3×10^{-4} einstein).

We have further investigated the light intensity dependence on the product selectivity in the photochemical CO_2 reduction. Figure 5 shows the light intensity dependence on the product ratio at a dilute concentration of *trans*(Cl)-Ru(bpy)$(CO)_2Cl_2$ (20 μM). The ratio of $CO/HCOO^-$ decreases by reducing the light intensity, that is, formation of $HCOO^-$ becomes dominant on the light at lower intensity. Since the concentration of 20 μM was selected to prevent the formation of the polymer which caused a dramatic decrease of the effective catalyst concentration in the solution, we could exclude the possibility that the polymeric species contribute the product selectivity. Considering that the low-intensity light induces the Ru-Ru bond formation, the most plausible key intermediate forming $HCOO^-$ would be the ruthenium dimer.

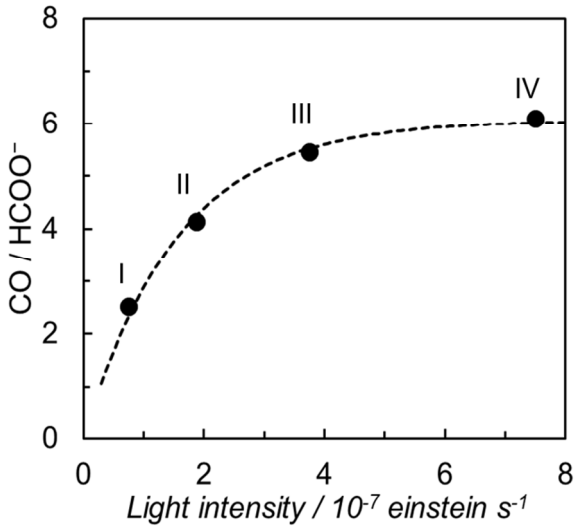

Figure 5. Light Intensity dependence on the product ratio of $CO/HCOO^-$ in DMA/water (9:1 v/v) solutions containing *trans*(Cl)-Ru(bpy)$(CO)_2Cl_2$ (20 μM), $[Ru(bpy)_3](PF_6)_2$ (0.50 mM) and BNAH (0.10 M) during photo-irradiation of λ > 400 nm light The photo-irradiation times are (I) 50 min, (II) 20 min, (III) 10 min and (IV) 5 min, respectively (total incident light: 2.3×10^{-4} einstein).

Mechanistic insight into product selectivity

The photochemical CO_2 reduction system consists of two parts: an electron relay cycle and a catalytic cycle (Scheme 3). In the electron relay cycle, the excited state of the photosensitizer (PS^*) and BNAH forms the encounter complex, where the electron transfer from BNAH to the PS^* occurs to produce the charge-separated state ($[PS^-....BNAH^{\cdot+}]$).[81,82] Dissociation of the encounter complex gives the free reduced photosensitizer (PS^-), which could supply the electrons to the catalyst. In Scheme 3, I_{ex} is the rate of incident photon, k_q is the quenching rate constant by BNAH, k_{r+nr} is total of the radiative and non-radiative rate constants of the PS*, α is the cage escape efficiency after the electron transfer from BNAH to the PS*,[82] β is the fraction of the back-electron transfer in the solvent cage ($\beta = 1-\alpha$), k_b is the quenching rate constant of the PS^-, k_i is the electron transfer rate constant from the PS^- to the ith form of the catalyst, and $[cat_i]$ is the concentration of the ith form of the catalyst. In the initial stage of the reaction, the quenching by BNA_2 can be ignored.[47] The steady-state concentration of the PS^- is evaluated as the function of the concentration of the catalyst (equation (2)) by applying the steady state approximation to Scheme 3:

$$[PS^-] = \frac{(\alpha\, k_q\, [\mathrm{BNAH}]\; I_{ex})/\{k_b(k_{r+nr}+k_q\, [\mathrm{BNAH}])\}}{1+\sum_i k_i[\mathrm{cat}_i]/k_b} \qquad (2)$$

According to equation (2), when the light intensity and the concentration of BNAH are constant, the steady-state concentration of the PS^- is affected by the catalyst concentration: $[PS^-]$ decreases as the catalyst concentration increases.

Scheme 3. The electron relay cycle and the catalytic cycle in the photochemical CO_2 reduction.

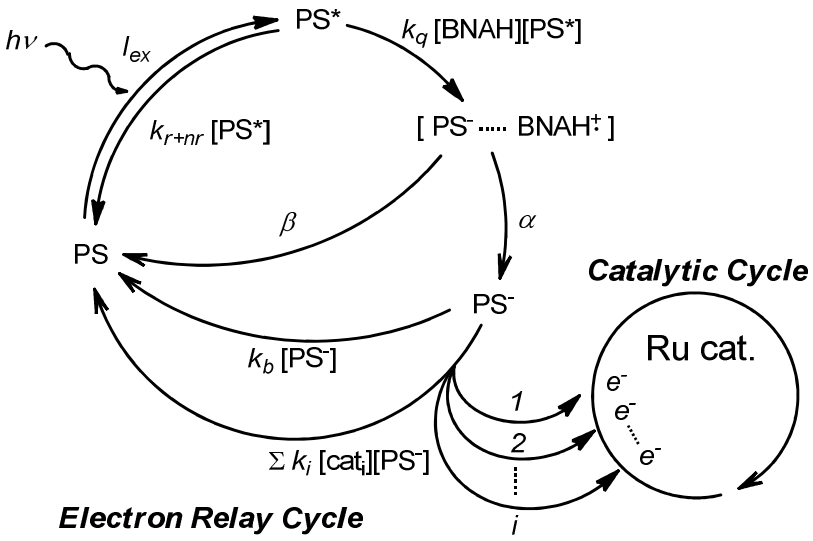

In the catalytic cycle, we have assumed that the dimeric complex produces formate while the monomeric complex produces CO by the reaction with CO_2 (Scheme 4). It has been reported that the one-electron-reduced catalyst (**Ru**$^+$) does not react with CO_2[48-56,69,70,83] but forms the dimer (**Ru**$^+$**−Ru**$^+$)[71,72]. Therefore the resting state in the catalytic cycle would be the **Ru**$^+$ species. In the low concentration region of the catalyst, it is possible for the catalyst to accept two electrons smoothly from the PS^-. On the other hand, in the high concentration region, the amount of the PS^- would not be enough for the catalyst to receive two electrons smoothly. In particular, in the photochemical reaction the electron transfer to the catalyst hardly occurs, and accordingly the **Ru**$^+$ remains unreacted.

Scheme 4. Plausible mechanism for CO_2 reduction.

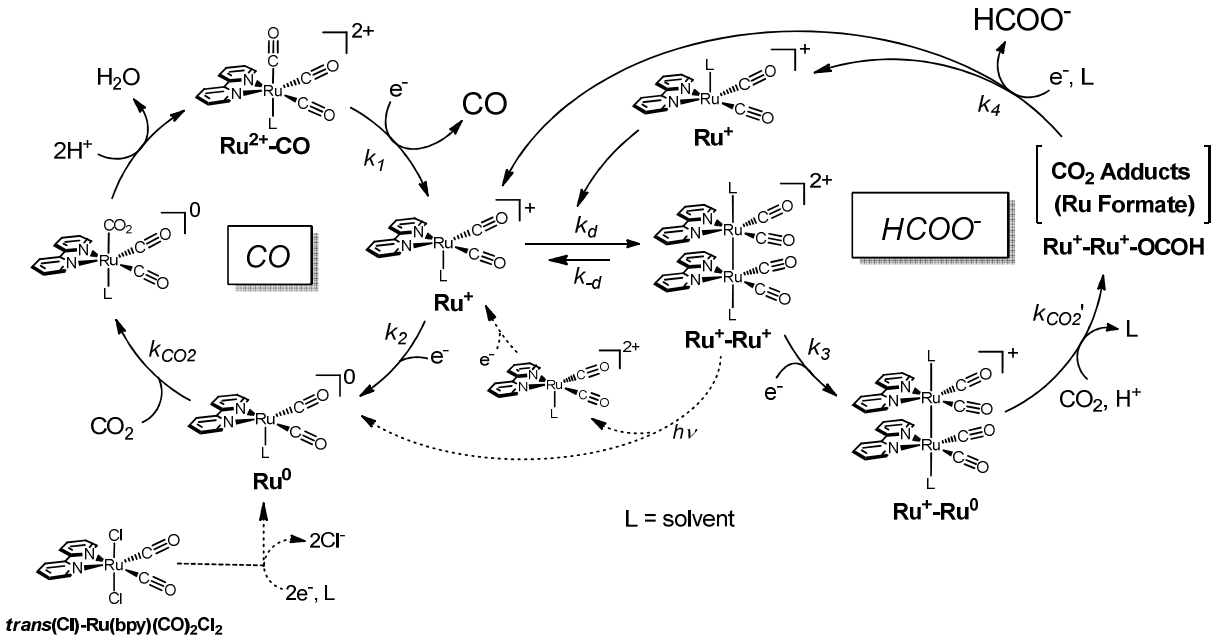

The valence of the ruthenium centre in the dimer possibly changes by the reaction with CO_2 and H^+. When the Ru(II) valence state forms, the Ru-Ru bond would dissociate into the monomeric species. In order to confirm the cleavage of the Ru-Ru bond, we examined the photocatalytic CO_2 reduction by $[Ru(bpy)(CO)_2Cl]_2$, which was separately prepared.[73] According to the reduction potential of $[Ru(bpy)(CO)_2Cl]_2$, which is estimated to be *ca.* −1.6 V vs. Ag/Ag^+ in DMA/water (9:1 v/v) (Figure S2 in Supporting Information), the electron transfer can thermodynamically occur from the reduced photosensitizer to the dimer. The reaction catalysed by 0.05 mM of $[Ru(bpy)(CO)_2Cl]_2$ (0.10 mM of the Ru unit) showed the very similar time-course profiles of CO and $HCOO^-$ to those by 0.10 mM of *trans*(Cl)-$Ru(bpy)(CO)_2Cl_2$ (Figure S3 in Supporting Information). The result supports that the formate production is accompanied with the cleavage of the Ru-Ru bond to reproduce the monomeric species. We have

carried out the photo-irradiation to a concentrated solution of $[Ru(bpy)(CO)_2Cl]_2$ (0.40 mM) in the Ar-saurated DMA/water without both the photosensitizer and the electron donor. The direct photo-irradiation to the dimer shows appearance of the broad absorption corresponding to the polymeric species, suggesting that disproportionation of the Ru(I)-Ru(I) dimer occurs (Scheme 4). The disproportionation of the dimer has been proposed in the isomerization from *trans*(Cl) to *cis*(Cl)-$Ru(bpy)(CO)_2Cl_2$ which is induced by addition of $NaBH_4$.[84] However, in the reaction condition in the presence of $[Ru(bpy)_3]^{2+}$ (0.50 mM) as the photosensitizer, direct photo-excitation of the dimer scarcely occur because most of the light is absorbed by the photosensitizer when the concentration of the dimer is low. In addition, we have observed that $[Ru(bpy)(CO)_2Cl]_2$ is stable against CO_2 in DMA/water in dark. Thus, it is thought that the formate production would start by electrical reduction of the $\mathbf{Ru^+-Ru^+}$.

The relationship between the concentration of the catalyst and the initial rates for CO and formate is evaluated by applying the steady state approximation to Scheme 4 and using equation (2). The equations for CO and formate are expressed as the following equation (3) and (4), respectively (See Supporting Information):

$$v_{CO} = v_0 + \frac{a[\mathrm{cat}]_t}{b\,[\mathrm{cat}]_t^{\,2} + c\,[\mathrm{cat}]_t + d} \qquad (3)$$

$$v_{HCOO^-} = v_0' + \frac{a'[\mathrm{cat}]_t^{\,2}}{b'[\mathrm{cat}]_t^{\,2} + c'[\mathrm{cat}]_t + d'} \qquad (4)$$

where v_{CO} and v_{HCOO^-} are the formation rates of CO and formate, which can be calculated by dividing mol of the products after the photo-irradiation for 30 min with the volume of the reaction solution (5.0 mL) and the time (1800 s); $[cat]_t$ is the initial concentration of *trans*(Cl)-$Ru(bpy)(CO)_2Cl_2$; γ is a proportional constant peculiar to the catalyst, $\gamma = [\mathbf{Ru^+}]/[cat]_t$; v_0 and v_0'

are the blank formation rates caused by $[Ru(bpy)_3]^{2+}$; a, b, c, d, a', b', c' and d' are the constant values as expressed by the following: $a = (k_2 k_{-d} \alpha k_q [\text{BNAH}] I_{ex} \gamma)/(k_{n+nr} + k_q [\text{BNAH}])$, $b = b' = 2 k_d k_3 \gamma^2$, $c = c' = 2 k_{-d} k_2 \gamma$, $d = k_b k_{-d} + (k_3 \alpha k_q [\text{BNAH}] I_{ex})/(k_{n+nr} + k_q [\text{BNAH}])$, $a' = (k_3 k_d \alpha k_q [\text{BNAH}] I_{ex} \gamma^2)/(k_{n+nr} + k_q [\text{BNAH}])$, $d' = k_b k_{-d}$,. The value of γ would be related to k_{CO_2} and k_{CO_2}', and the higher value of γ would indicate the higher reaction rate of the two-electron-reduced catalyst with CO_2 and H^+.

In Figure 3 top, the curve fitting according to equation (3) gives the parameters: $v_0 = 1.2\times10^{-6}$ M s^{-1}, $a/d = 1.1$ s^{-1}, $b/d = 1.1\times10^{9}$ M^{-2}, $c/d = 9.1\times10^{4}$ M^{-1}. The simulation curve well reproduces the experimental behaviour where the rate increases as the catalyst concentration increases by 20−30 μM and decreases at more than 30 μM. Equation (4) can be simplified when the term of d' is negligible (Figure S9 in Supporting Information):

$$v_{HCOO^-} = v_0' + \frac{a'[\text{cat}]_t}{b'[\text{cat}]_t + c'} \qquad (5)$$

By considering v_0' = 4.2×10^{-7} M s^{-1}, the double-reciprocal plots of the rate of formate production versus the concentration of *trans*(Cl)-Ru(bpy)$(CO)_2Cl_2$ give $a'/c' = 0.10$ s^{-1}, $b'/c' = 1.8\times10^{4}$ M^{-1} (Figure 6). These simulation curves based on equation (3) and (5) agree well with the experimental plots in Figure 3 top, and also reproduce the results for the selectivity in Figure 3 bottom.

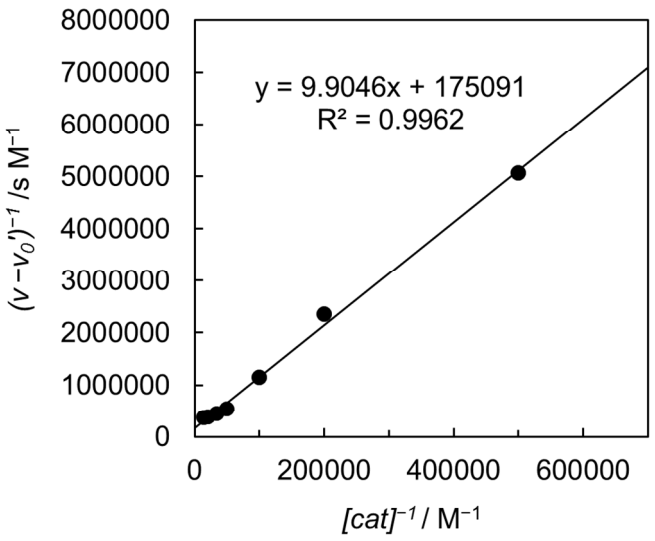

Figure 6. Double-reciprocal plots of the rate of the formate production versus the concentration of *trans*(Cl)-Ru(bpy)$(CO)_2Cl_2$.

In the equations (3), (4) and (5), the following relationships should be satisfied; $b/c = b'/c'$ and $a/c = a'/b'$. From equations (3) and (5), b/c and b'/c' are estimated to be 1.3×10^4 M^{-1} and 1.8×10^4 M^{-1}, and a/c and a'/b' to be 1.2×10^{-5} M s^{-1} and 0.6×10^{-5} M s^{-1}, respectively. The results from the curve fittings satisfy with the theoretical requirements. Furthermore, a/c and a'/b' are expressed as equation (6) and the value can be estimated using $k_q = 2.6 \times 10^8$ $M^{-1}s^{-1}$, $k_{r+nr} = 1.2 \times 10^6$ s^{-1} and $\alpha I_{ex} = 3.3\times10^{-5}$ M s^{-1}, which are obtained from the Stern-Volmer plot, the emission lifetime of the excited $[Ru(bpy)_3]^{2+}$ and the simulation curve of the decrease of BNAH, respectively.[47]

$$\frac{\alpha\ k_q\,[\mathrm{BNAH}]\ I_{ex}}{2(k_{r+nr}+k_q\,[\mathrm{BNAH}])} = 1.6 \times 10^{-5}\ \mathrm{M\ s^{-1}} \qquad (6)$$

This value is consistent with a/c and a'/b' estimated from equation (3) and (5), indicating that the kinetic analyses strongly support the proposed mechanism.

Photochemical CO_2 reduction using $[Ru(4dmbpy)_3]^{2+}$ as photosensitizer

As the photosensitizer in the photochemical CO_2 reduction, we have used $[Ru(bpy)_3]^{2+}$ whose first reduction potential is −1.68 V vs. Ag/Ag^+ in DMA/water (9:1 v/v).[47] In order to investigate the effect of the photosensitizer on the product selectivity, we use $[Ru(4dmbpy)_3]^{2+}$ (4dmbpy = 4,4'-dimethyl-2,2'-bipyridine) instead of $[Ru(bpy)_3]^{2+}$. $[Ru(4dmbpy)_3]^{2+}$ has more negative reduction potential of −1.77 V vs. Ag/Ag^+ (Figure S4) than that of $[Ru(bpy)_3]^{2+}$, indicating that $[Ru(4dmbpy)_3]^{2+}$ works as a powerful reductant after the photo-induced electron transfer from BNAH is completed. However, the more negative potential of $[Ru(4dmbpy)_3]^{2+}$ makes the quenching rate constant by BNAH more inefficient ($k_q \sim 1.7\times10^7$ $M^{-1}s^{-1}$)[85] than that of $[Ru(bpy)_3]^{2+}$ ($k_q = 2.6\times10^8$ $M^{-1}s^{-1}$)[47] by one digit or more.

Figure 7 shows the relationship between the concentration of the catalyst and the initial rates for the CO and formate production using $[Ru(4dmbpy)_3]^{2+}$. The simulation curves based on equation (3) and (4) well reproduce the experimental plots where formate shows an induction region for the production at very low concentration, and CO shows the plots of a downward convex shape at high concentration. From the curve fittings in Figure 7 and the blank experiment caused by $[Ru(4dmbpy)_3]^{2+}$ the parameters are given as: $v_0 = 1.5\times10^{-6}$ M s^{-1}, $a/d = 2.5$ s^{-1}, $b/d = 1.0\times10^{10}$ M^{-2}, $c/d = 7.7\times10^5$ M^{-1}, $v_0' = 2.2\times10^{-7}$ M s^{-1}, $a'/d' = 1.5\times10^4$ $M^{-1}s^{-1}$, $b'/d' = 8.4\times10^9$ M^{-2}, $c'/d' = 2.1\times10^5$ M^{-1}. While the values of b/c and b'/c' estimated to be 1.3×10^4 M^{-1} and 4.0×10^4 M^{-1} are similar to those using $[Ru(bpy)_3]^{2+}$ ($b/c = 1.3\times10^4$ M^{-1} and $b'/c' = 1.8\times10^4$ M^{-1} in Figure 3), the values of a/c and a'/b' estimated to be 3.3×10^{-6} M s^{-1} and 1.8×10^{-6} M s^{-1} are smaller than those using $[Ru(bpy)_3]^{2+}$ ($a/c = 1.2\times10^{-5}$ M s^{-1} and $a'/b' = 0.6\times10^{-5}$ M s^{-1} in Figure 3). Assuming that the cage escape efficiency is same with that for $[Ru(bpy)_3]^{2+}$ ($\alpha I_{ex} = 3.3\times10^{-5}$

M s^{-1}), the value of equation (6) is estimated to be 9.4×10^{-6} M s^{-1} using the quenching rate constant of $[Ru(4dmbpy)_3]^{2+}$. Thus, the smaller values of *a*/*c* and *a'*/*b'* estimated in Figure 7 well reflects the smaller quenching rate constant (k_q) of $[Ru(4dmbpy)_3]^{2+}$. In addition, the maximum selectivity in the products ratio attains *ca.* 13 at the concentration of 3 μM of the catalyst, indicating that the selectivity of CO is higher than that observed in Figure 3. The result implies that the reduction potential of the **Ru**$^{+}$ is more negative than that of the **Ru**$^{2+}$**-CO** in Scheme 4, and that the powerful reductant smoothly supplies the second electron to the **Ru**$^{+}$ in the low concentration region of the catalyst.

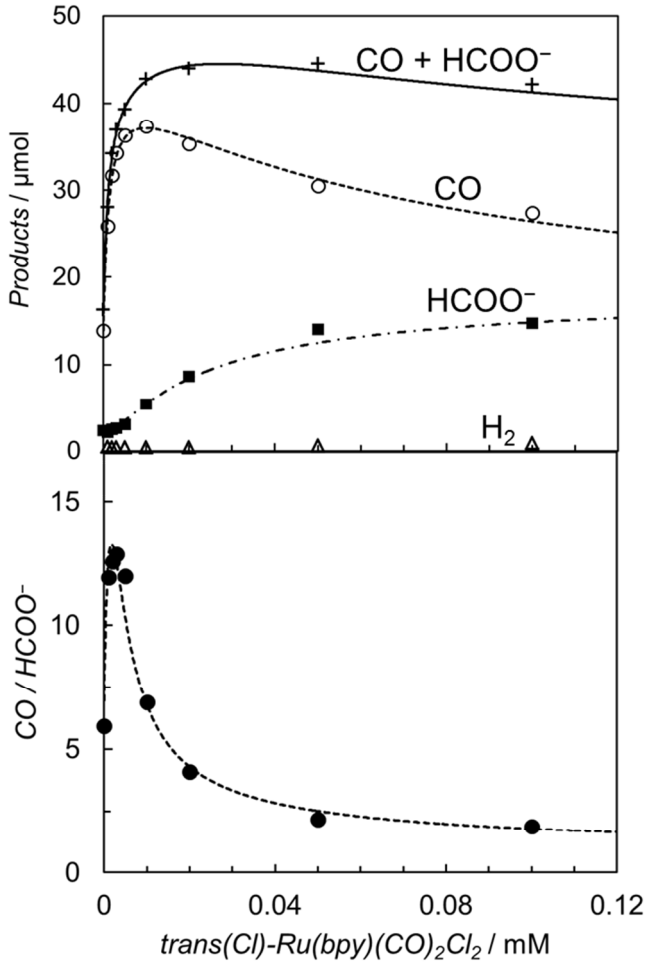

Figure 7. (Top) Plots of the reduction products after 30 min of the photo-irradiation (400 W Hg lamp, $\lambda > 400$ nm) versus the concentration of *trans*(Cl)-Ru(bpy)$(CO)_2Cl_2$ in CO_2-saturated DMA/water (9:1, v/v) in the presence of $[Ru(4dmbpy)_3](PF_6)_2$ (0.50 mM), BNAH (0.10 M): CO (○), $HCOO^-$ (■) , H_2 (Δ) and CO + $HCOO^-$ (+). (Bottom) Plots of CO/ $HCOO^-$ ratio versus the concentration of *trans*(Cl)-Ru(bpy)$(CO)_2Cl_2$. The curves represent the theoretical fittings based on the kinetic analyses (see equations (3) and (4)).

Selective CO formation in photochemical CO_2 reduction using *trans*(Cl)-Ru(6Mes-bpy)$(CO)_2Cl_2$

While we have succeeded in elucidating the product selectivity with the kinetic analyses, we have not yet directly detected the dimer during the CO_2 reduction reaction by mean of the spectroscopic methods such as UV-vis absorption and ESI-MS. It is because the absorption band of the dimer is overlapped with that of $[Ru(bpy)_3]^{2+}$ and the absorption coefficient of the dimer at 450 nm is around one-quarter smaller than that of $[Ru(bpy)_3]^{2+}$ (Figure 4b).[86] Even if all of *trans*(Cl)-Ru(bpy)$(CO)_2Cl_2$ (0.1 mM) transforms to the Ru(I)-Ru(I) dimer during the photochemical reaction, the contribution of the dimer would be only 2.5% of the whole absorption. In addition, the polymerization easily occurs even in the CO_2-saturated DMA/water when a high concentration (>0.2 mM) of the *trans*(Cl)-Ru(bpy)$(CO)_2Cl_2$ is used. The attempt to detect the intermediate by ESI-MS has also failed so far due to the less stability in the ionized process on the measurement. Thus, we have changed the strategy to verify the proposed mechanism: we have synthesized a novel ruthenium complex, *trans*(Cl)-Ru(6Mes-bpy)$(CO)_2Cl_2$, which has mesityl groups at 6,6'-positions of the bipyridine ligand to suppress the dimer formation, and have investigated the product selectivity in the photocatalytic CO_2 reduction.

The synthesis is described in the experimental section. The reduction potential of *trans*(Cl)-Ru(6Mes-bpy)$(CO)_2Cl_2$ (−1.56 V vs. Ag/Ag^+ in DMA/water (9:1 v/v), Figure S7 in Supporting Information), is similar to that of *trans*(Cl)-Ru(bpy)$(CO)_2Cl_2$, indicating that the mesityl groups do not strongly affect the electronic structure. This also suggests that electron transfer reaction from the reduced photosensitizer to *trans*(Cl)-Ru(6Mes-bpy)$(CO)_2Cl_2$ similarly occurs as *trans*(Cl)-Ru(bpy)$(CO)_2Cl_2$ does. Before performing the photocatalytic CO_2 reduction, we have checked that *trans*(Cl)-Ru(6Mes-bpy)$(CO)_2Cl_2$ does not form the dimer by monitoring

the absorption spectral changes of the solutions containing the ruthenium complex, $[Ru(bpy)_3]^{2+}$ and BNAH during the photo-irradiation under Ar atmosphere. In contrast to *trans*(Cl)-$Ru(bpy)(CO)_2Cl_2$ as shown in Figure 4a, no absorption band corresponding to the polymeric complex is observed as shown in Figure 8, indicating that the bulky substituents at the 6,6'-positions of the bipyridyl ligand suppress the formation of the Ru-Ru bond. The differential absorption spectra show the small spectral changes with a broad shoulder between 550 and 600 nm (see the inset in Figure 8). They are comparable with the spectral changes in the electrolysis (Figure S8 in the Supporting Information), because the spectral changes in the photo-reaction (Figure 8) overlap the absorption of the photosensitizer and the electron donor. The spectral changes in photo-reaction would be due to formation of the one-electron reduced but non-dimerised species of the ruthenium complex.

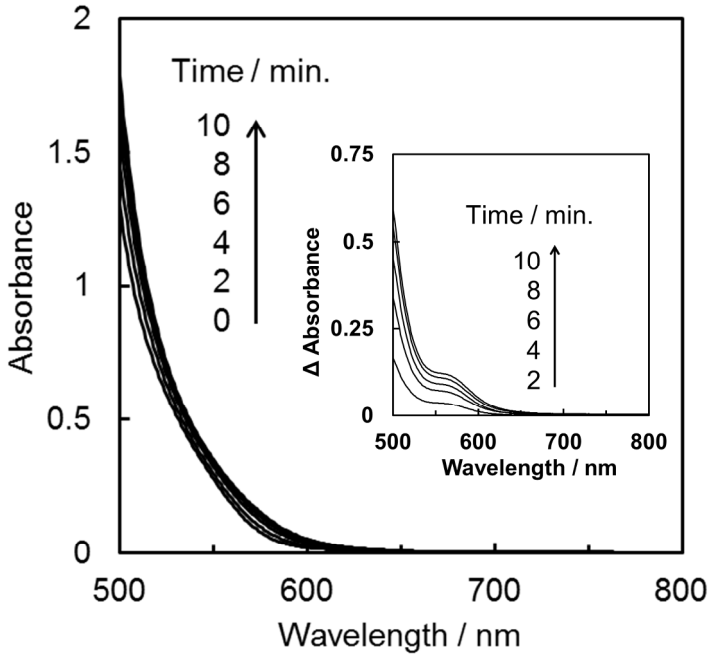

Figure 8. Absorption spectral changes of the DMA/water (9:1, v/v) solution containing *trans*(Cl)-Ru(6Mes-bpy)$(CO)_2Cl_2$ (0.20 mM), $[Ru(bpy)_3]^{2+}$ (0.50 mM) and BNAH (0.10 M) during the photo-irradiation of $\lambda > 400$ nm light with intensity of 7.5×10^{-7} einstein s^{-1} under Ar atmosphere. The inset shows the differential absorption spectra (optical path length: 10 mm).

The photochemical CO_2 reduction has been carried out using *trans*(Cl)-Ru(6Mes-bpy)$(CO)_2Cl_2$ as the catalyst in the DMA/water (9:1 v/v) solution containing $[Ru(bpy)_3]^{2+}$ (0.50 mM) as the photosensitizer and BNAH (0.10 M) as the electron donor. The relationships between the concentration of the catalyst and the amounts of CO and formate are shown in Figure 9. In contrast with Figure 3, Figure 9 shows that CO mainly forms accompanied with a small amount of formate. The formate production is independent of the catalyst concentration,

indicating that the formate comes from the blank reaction by $[Ru(bpy)_3]^{2+}$. The plots of the CO production versus the catalyst concentration are well fitted with the kinetic analysis based on the mechanism without considering the dimer formation. When the dimer formation is negligible in Scheme 3 and 4, the production rate for CO is expressed as equation (7) (Supporting Information):

$$v_{CO} = v_0 + \frac{a''[\text{cat}]_t}{b''[\text{cat}]_t + c''} \qquad (7)$$

where *a"*, *b"* and *c*" are the constant values as expressed by the following: $a'' = k_2\, \alpha\, k_q\, [\text{BNAH}]\, I_{ex}\, \gamma$, $b'' = 2\, k_2\, (k_{n+nr} + k_q\, [\text{BNAH}])\gamma$, $c'' = k_b\, (k_{n+nr} + k_q\, [\text{BNAH}])$. The curve fitting based on equation (6) gives the parameters: $v_0 = 2.4\times10^{-6}$ M s^{-1}, $a''/b'' = 0.85\times10^{-5}$ M s^{-1}, $c''/b'' = 2.7\times10^{-5}$ M. The value of a''/b'' is also consistent with the value (1.6×10^{-5} M s^{-1}) in equation (6). Thus, *trans*(Cl)-Ru(6Mes-bpy)$(CO)_2Cl_2$, which does not form the dimer, affords CO selectively in the photocatalytic CO_2 reduction.[87]

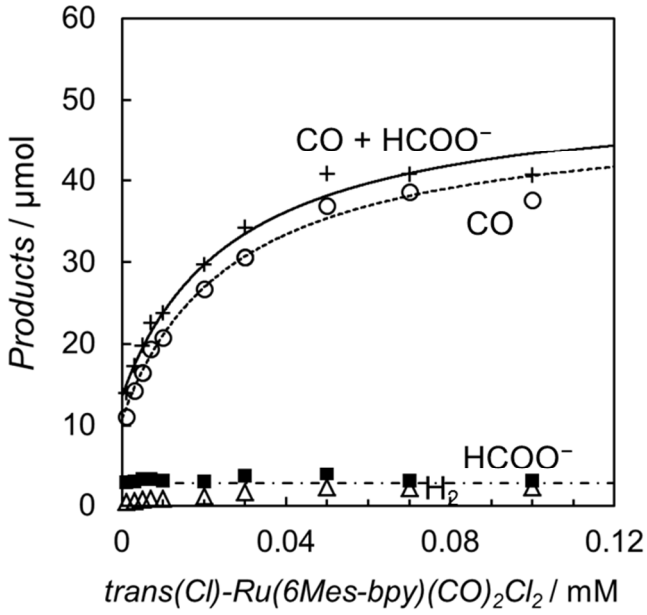

Figure 9. Plots of the reduction products after 15 min of the photo-irradiation (400 W Hg lamp, $\lambda > 400$ nm) versus the concentration of *trans*(Cl)-Ru(6Mes-bpy)$(CO)_2Cl_2$ in CO_2-saturated DMA/water (9:1, v/v) in the presence of $[Ru(bpy)_3](PF_6)_2$ (0.50 mM), BNAH (0.10 M): CO (○), $HCOO^-$ (■) , H_2 (Δ) and CO + $HCOO^-$ (+).The curve for CO represents the theoretical fittings based on the kinetic analysis (see equations (7)).

Deronzier and Ziessel *et al*. reported that the electrochemical CO_2 reduction using the ruthenium polymer such as $[Ru(bpy)(CO)_2]_n$ affords CO selectively.[63-68] These reports seem to be inconsistent with our results. It should be noted that the electrochemical reactions are different from the photochemical catalyses. In the electrochemical reaction, electrons can be efficiently supplied from the electrodes into the catalysts, resulting in that the valences of the most ruthenium complexes are reduced to 0 or less, −1.[68] To the contrary, in the photochemical catalyses discussed in this report, reduction of the catalysts occurs *via* the reaction between the reduced species of the photosensitizer and the catalyst. In the catalyses, there are various possible

intermediates and reaction paths. The major reaction pathway is strongly dependent on the reaction (e.g., photochemical or electrochemical reaction) and the conditions (e.g., solvents, pH). The experimental results in this report suggest that the Ru(I) species of the dimer would play an important role for the formate production in the reaction mechanism. It still remains unknown how the Ru(I) dimer can selectively produce formate from CO_2. Further computational studies for the process are now underway.

Conclusion

We have carried out the photochemical CO_2 redcution catalyzed by *trans*(Cl)-$Ru(bpy)(CO)_2Cl_2$, and have unexpectedly found that the product ratio of CO to formate depends on the concentration of the catalyst. In order to expain the behaivor of the $CO/HCOO^-$ selectivity, we have proposed a new reaction mechanism containing formation of the catalyst dimer which selectively produces formate. The mechanism has strongly been supported by the kinetic analyses, the catalyses by $[Ru(bpy)(CO)_2Cl]_2$ and the light intensity dependence of the $CO/HCOO^-$ selectivity. The Mechanism for the photocatalytic CO_2 reduction consists of the electron relay cycle and the catalytic CO_2 reduction cycle. The former is the process in which the reduced photosensitizer (PS^-) supplies electrons into the catalyst, and the latter is the steps where the ruthenium complexes catalytically reduce CO_2 by using the supllied electrons. At the high catalyst concentration, the electron relay system would be rate-detemining because the catalysis becomes faster than the electron supply. Under this condition, the ruthenium catalyst cannot be sufficiently received electrons; the one-electron reduced species of the catalyst cannot accept

more electrons, and it forms the dimer which produces $HCOO^-$. Therefore as the catalyst concentration increases, the product selectivity ($CO/HCOO^-$) decreases. As reducing the light intensity, the concentration of PS^- also decreases, resulting in the same effect as the high concentration of the catalyst. The mechanism also elucidate the photo-irradiation time dependence on the CO_2 reduction: the CO production reaches saturation. At longer reaction time, the electron donor BNAH is consumed to decrease the concentration of PS^-. At the situation, the one-electron reduced species of the catalyst cannot accept more electrons and forms the catalyst dimer, making the CO production decrease. However, the $HCOO^-$ formation continues till exhausting the electron donor. We have further designed and synthesized a novel ruthenium complex, *trans*(Cl)-Ru(6Mes-bpy)$(CO)_2Cl_2$, which has a bulky ligand to eliminate the contribution of the dimer. By suppressing the dimer formation, the photochemical CO_2 reduction produces CO selectively. In the photocatalytic systems for the CO_2 reduction by ruthenium complexes, to the best of our knowledge, this system is the first case producing CO selectively. This finding does not only elucidate the reaction mechanisms for the photocatalytic CO_2 reduction but also leads us to design more effective metal complexes for the catalyses.

Acknowledgement

This work was supported by the PRESTO Program of JST. We thank Mr. Masaya Kamiya and Mr. Kousuke Matsuura for experimental supports.

References and Notes

1. G. A. Olah, G. K. S. Prakash, A. Goeppert, *J. Am. Chem. Soc.*, 2011, **133**, 12881-12898.
2. T. R. Cook, D. K. Dogutan, S. Y. Reece, Y. Surendranath, T. S. Teets, D. G. Nocera, *Chem. Rev.,* 2010, **110**, 6474–6502.
3. J. H. Alstrum-Acevedo, M. K. Brennaman, T. J. Meyer, *Inorg. Chem.,* 2005, **44**, 6802-6827.
4. H. Arakawa, M. Aresta, J. N. Armor, M. A. Barteau, E. J. Beckman, A. T. Bell, J. E. Bercaw, C. Creutz, E. Dinjus, D. A. Dixon, K. Domen, D. L. DuBois, J. Eckert, E. Fujita, D. H. Gibson, W. A. Goddard, D. W. Goodman, J. Keller, G. J. Kubas, H. H. Kung, J. E. Lyons, L. E. Manzer, T. J. Marks, K. Morokuma, K. M. Nicholas, R. Periana, L. Que, J. Rostrup-Nielson, W. M. H. Sachtler, L. D. Schmidt, A. Sen, G. A. Somorjai, P. C. Stair, B. R. Stults, W. Tumas, *Chem. Rev.,* 2001, **101**, 953-996.
5. K. Kobayashi, K. Tanaka, *Phys. Chem. Chem. Phys.,* 2014, **16**, 2240-2250.
6. D. L. DuBois, *Inorg. Chem.,* 2014, **53***,* 3955-3960.
7. A. M. Appel, J. E. Bercaw, A. B. Bocarsly, H. Dobbek, D. L. DuBois, M. Dupuis, J. G. Ferry, E. Fujita, R. Hille, P. J. A. Kenis, C. A. Kerfeld, R. H. Morris, C. H. F. Peden, A. R. Portis, S. W. Ragsdale, T. B. Rauchfuss, J. N. H. Reek, L. C. Seefeldt, R. K. Thauer, G. L. Waldrop, *Chem. Rev.,* 2013, **113**, 6621−6658.
8. C. D. Windle, R. N. Perutz, *Coord. Chem. Rev*., 2012, **256**, 2562-2570.
9. T. Yui, Y. Tamaki, K. Sekizawa, O. Ishitani, *Top. Curr. Chem*., 2011, **303**, 151-184.
10. H. Takeda, O. Ishitani, *Coord. Chem. Rev.,* 2010, **254**, 346-354.
11. K. Tanaka, *Chem. Rec.,* 2009, **9**, 169-186.
12. A. J. Morris, G. J. Meyer, E. Fujita, *Acc. Chem. Res.,* 2009, **42**, 1983-1994.
13. E. E. Benson, C. P. Kubiak, A. J. Sathrum, J. M. Smieja, *Chem. Soc. Rev.,* 2009, **38**, 89-99.

14. J.-M. Savéant, *Chem. Rev.,* 2008, **108**, 2348-2378.

15. P. G. Jessop, T. Ikariya, R. Noyori, *Chem. Rev.,* 1995, **95**, 259-272.

16. M. D. Sampson, A. D. Nguyen, K. A. Grice, C. E. Moore, A. L. Rheingold, C. P. Kubiak, *J. Am. Chem. Soc.,* 2014, **136**, 5460−5471.

17. H. Takeda, H. Koizumi, K. Okamoto, O. Ishitani, *Chem. Commun.,* 2014, **50**, 1491-1493.

18. M. Bourrez, F. Molton, S. Chardon-Noblat, A. Deronzier, *Angew. Chem. Int. Ed.,* 2011, **50**, 9903-9906.

19. C. Costentin, S. Drouet, M. Robert, J.-M. Savéant, *Science,* 2012, **338**, 90-94.

20. J. Grodkowski, D. Behar, P. Neta, P. Hambright, *J. Phys. Chem. A,* 1997, **101**, 248-254.

21. M. Hammouche, D. Lexa, M. Momenteau, J.-M. Savéant, *J. Am. Chem. Soc.,* 1991, **113**, 8455-8466.

22. R. Ziessel, J. Hawecker, J.-M. Lehn, *Helv. Chim. Acta,* 1986, **69**, 1065-1084.

23. S. Matsuoka, K. Yamamoto, T. Ogata, M. Kusaba, N. Nakashima, E. Fujita, S. Yanagida, *J. Am. Chem. Soc.,* 1993, **115**, 601-609.

24. A. H. P. Tinnemans, T. P. M. Koster, D. H. M. W. Thewissen, A. Mackor, *Recl. Trav. Chim. Pays-Bas,* 1984, **103**, 288-295.

25. M. Rudolph, S. Dautz, E.-G. Jäger, *J. Am. Chem. Soc.,* 2000, **122**, 10821-10830.

26. M. A. Mndez, P. Voyame, H. H. Girault, *Angew. Chem. Int. Ed.,* 2011, **50**, 7391-7394.

27. J. L. Grant, K. Goswami, L. O. Spreer, J. W. Otvos, M. Calvin, *J. Chem. Soc., Dalton Trans.,* 1996, 2581-2583.

28. M. L. Clark, K. A. Grice, C. E. Moore, A. L. Rheingold, C. P. Kubiak, *Chem. Sci.*, 2014, **5**, 1894-1900.

29. S. C. Rasmussen, M. M. Richter, E. Yi, H. Place, K. J. Brewer, *Inorg. Chem.,* 1990, **29**, 3926-3932.

30. C. M. Bolinger, N. Story, B. P. Sullivan, T. J. Meyer, *Inorg. Chem.,* 1988, **27**, 4582-4587.

31. P. R. Bernatis, A. Miedaner, R. C. Haltiwanger, D. L. DuBois, *Organometallics,* 1994, **13**, 4835-4843.

32. D. L. DuBois, A. Miedaner, R. C. Haltiwanger, *J. Am. Chem. Soc.,* 1991, **113**, 8153-8164.

33. D. L. DuBois, A. Miedaner, *J. Am. Chem. Soc.,* 1987, **109**, 113-117.

34. Y. Kou, Y. Nabetani, D. Masui, T. Shimada, S. Takagi, H. Tachibana, H. Inoue, *J. Am. Chem. Soc.,* 2014, **136**, 6021−6030.

35. T. Morimoto, T. Nakajima, S. Sawa, R. Nakanishi, D. Imori, O. Ishitani, *J. Am. Chem. Soc.,* 2013, **135**, 16825-16828.

36. T. Morimoto, C. Nishiura, M. Tanaka, J. Rohacova, Y. Nakagawa, Y. Funada, K. Koike, Y. Yamamoto, S. Shishido, T. Kojima, T. Saeki, T. Ozeki, O. Ishitani, *J. Am. Chem. Soc.,* 2013, **135**, 13266-13269.

37. Y. Tamaki, K. Koike, T. Morimoto, Y. Yamazaki, O. Ishitani, *Inorg. Chem.,* 2013, **52**, 11902-11909.

38. Y. Tamaki, K. Koike, T. Morimoto, O. Ishitani, *J. Catal.,* 2013, **304**, 22-28.

39. H. Takeda, K. Koike, H. Inoue, O. Ishitani, *J. Am. Chem. Soc.*, 2008, **130**, 2023-2031.

40. B. Gholamkhass, H. Mametsuka, K. Koike, T. Tanabe, M. Furue, O. Ishitani, *Inorg. Chem.,* 2005, **44**, 2326-2336.

41. Y. Hayashi, S. Kita, B. S. Brunschwig, E. Fujita, *J. Am. Chem. Soc.* 2003, **125**, 11976-11987.

42. J. Hawecker, J.-M. Lehn, R. Ziessel, *Helv. Chim. Acta,* 1986, **69**, 1990-2012.

43. J. Chauvin, F. Lafolet, S. Chardon-Noblat, A. Deronzier, M. Jakonen, M. Haukka, *Chem. Eur. J.,* 2011, **17**, 4313-4322.

44. M. R. M. Bruce, E. Megehee, B. P. Sullivan, H. H. Thorp, T. R. O'TooIe, A. Downard, J. R. Pug, T. J. Meyer, *Inorg. Chem.,* 1992, **31**, 4864-4873.

45. S. Sato, T. Morikawa, T. Kajino, O. Ishitani, *Angew. Chem. Int. Ed.,* 2013, **52**, 988-992.

46. P. Kang, C. Cheng, Z. Chen, C. K. Schauer, T. J. Meyer, M. Brookhart, *J. Am. Chem. Soc.,* 2012, **134**, 5500-5503.

47. Y. Kuramochi, M. Kamiya, H. Ishida, *Inorg. Chem.,* 2014, **53**, 3326-3332.

48. P. Voyame, K. E. Toghill, M. A. Méndez, H. H. Girault, *Inorg. Chem.,* 2013, **52**, 10949-10957.

49. Y. Tamaki, T. Morimoto, K. Koike, O. Ishitani, *Proc. Natl. Acad. Sci. U. S. A.,* 2012, **109**, 15673-15678.

50. J. R. Pugh, M. R. M. Bruce, B. P. Sullivan, T. J. Meyer, *Inorg. Chem.,* 1991, **30**, 86-91.

51. H. Ishida, T. Terada, K. Tanaka, T. Tanaka, *Inorg. Chem.,* 1990, **29**, 905-911.

52. H. Ishida, K. Tanaka, T. Tanaka, *Chem. Lett.,* 1988, 339-342.

53. H. Ishida, K. Tanaka, T. Tanaka, *Chem. Lett.,* 1987, 1035-1038.

54. H. Ishida, H. Tanaka, K. Tanaka, T. Tanaka, *J. Chem. Soc., Chem. Commun.,* 1987, 131-132.

55. H. Ishida, K. Tanaka, T. Tanaka, *Organometallics,* 1987, **6**, 181-186.

56. H. Ishida, K. Tanaka, T. Tanaka, *Chem. Lett.,* 1985, 405-406.

57. J. Hawecker, J.-M. Lehn, R. Ziessel, *J. Chem. Soc., Chem. Commun.,* 1985, 56-58.

58. K. Maeda, K. Sekizawa, O. Ishitani, *Chem. Commun.,* 2013, **49**, 10127-10129.

59. T. M. Suzuki, H. Tanaka, T. Morikawa, M. Iwaki, S. Sato, S. Saeki, M. Inoue, T. Kajino, T. Motohiro, *Chem. Commun.,* 2011, **47**, 8673-8675.

60. S. Sato, T. Arai, T. Morikawa, K. Uemura, T. M. Suzuki, H. Tanaka, T. Kajino, *J. Am. Chem. Soc.,* 2011, **133**, 15240-15243.

61. T. Arai, S. Sato, K. Uemura, T. Morikawa, T. Kajino, T. Motohiro, *Chem. Commun.,* 2010, **46**, 6944-6946.

62. S. Sato, T. Morikawa, S. Saeki, T. Kajino, T. Motohiro, *Angew. Chem., Int. Ed.,* 2010, **49**, 5101-5105.

63. (a) S. Chardon-Noblat, C. H. Cripps, A. Deronzier, J. S. Field, S. Gouws, R. J. Haines, F. Southway, *Organometallics*, 2001, **20**, 1668-1675; (b) S. Chardon-Noblat, C. P. Da, A. Deronzier, M. Haukka, T. A. Pakkanen, R. Ziessel, *J. Electroanal. Chem.,* 2000, **490**, 62-69.

64. S. Chardon-Noblat, A. Deronzier, R. Ziessel, D. Zsoldos, *J. Electroanal. Chem.,* 1998, **444**, 253-260.

65. S. Chardon-Noblat, A. Deronzier, R. Ziessel, D. Zsoldos, *Inorg. Chem.,* 1997, **36**, 5384-5389.

66. S. Chardon-Noblat, M. N. Collomb-Dunand-Sauthier, A. Deronzier, R. Ziessel, D. Zsoldos, *Inorg. Chem.,* 1994, **33**, 4410-4412.

67. M. N. Collomb-Dunand-Sauthier, A. Deronzier, R. Ziessel, *Inorg. Chem.,* 1994, **33***,* 2961-2967.

68. M. N. Collomb-Dunand-Sauthier, A. Deronzier, R. Ziessel, *J. Chem. Soc., Chem. Commun.,* 1994, 189-191.

69. H. Ishida, K. Fujiki, T. Ohba, K. Ohkubo, K. Tanaka, T. Terada, T. Tanaka, *J. Chem. Soc., Dalton Trans.,* 1990, 2155-2160.

70. J.-M. Lehn, R. Ziessel, *J. Organomet. Chem.,* 1990, **382**, 157-173.

71. S. Chardon-Noblat, A. Deronzier, D. Zsoldos, R. Ziessel, M. Haukka, T. Pakkanen, T. Venalainen, *J. Chem. Soc., Dalton Trans.,* 1996, 2581-2583.

72. S. Myllynen, M. Wasberg, *J. Electroanal. Chem*., 2008, **623**, 93-101.

73. M. Haukka, J. Kiviaho, M. Ahlgren, T. A. Pakkanen, *Organometallics,* 1995, **14**, 825-833.

74. A. Paul, D. Connolly, M. Schulz, M. T. Pryce, J. G. Vos, *Inorg. Chem.,* 2012, **51**, 1977-1979.

75. P. A. Anderson, G. B. Deacon, K. H. Haarmann, F. R. Keene, T. J. Meyer, D. A. Reitsma, B. W. Skelton, G. F. Strouse, N. C. Thomas, J. A. Treadway, A. H. Whit, *Inorg. Chem.,* 1995, **34**, 6145-6157.

76. K. Suzuki, A. Kobayashi, S. Kaneko, K. Takehira, T. Yoshihara, H. Ishida, Y. Shiina, S. Oishi, S. Tobita, *Phys. Chem. Chem. Phys.,* 2009, **11***,* 9850-9860.

77. M. Schmittel, A. Ganz, W. A. Schenk, M. Z. Hagel, *Naturforsch*, 1999, **54b**, 559-564.

78. D. Mauzerall, F. H. Westheimer, *J. Am. Chem. Soc.,* 1955, **77**, 2261-2264.

79. M. N. Collomb-Dunand-Sauthier, A. Deronzier, R. Ziessel, *J. Electroanal. Chem.,* 1991, **319**, 347-353.

80. M. N. Collomb-Dunand-Sauthier, A. Deronzier, R. Ziessel, *J. Electroanal. Chem.,* 1993, **350**, 43-55.

81. G. J. Kavarnos, *Fundamentals of Photoinduced Electron Transfer*. Wiley-VCH: Weinheim, 1993.

82. M. Z. Hoffman, *J. Phys. Chem.,* 1988, **92**, 3458-3464.

83. E. Fujita, M. Chou, K. Tanaka, *Appl. Organomet. Chem.,* 2000, **14**, 844-846.

84. Y. Kuramochi, Y. Ito, H. Ishida, *Eur. J. Inorg. Chem.,* 2012, **2012**, 1167-1170.

85. The quenching rate constant was estimated by using the Stern-Volmer constant of K_{SV} = 13 M^{-1} (Figure S5) and the emission lifetime of $[Ru(4dmbpy)_3]^{2+}$ assuming to be 766 ns. See reference 49.

86. S. Myllynen, M. Wasberg, M. Haukka, *J. Electroanal. Chem.,* 2006, **586**, 217-224.

87. We have also examined the photochemical CO_2 reduction catalysed by *trans*(Cl)-Ru(4dmbpy)$(CO)_2Cl_2$ whose first reduction potential is −1.58 V vs. Ag/Ag^+ in DMA/water (9:1 v/v). The concentration dependence of the catalyst on the product selectivity is similar to that of *trans*(Cl)-Ru(bpy)$(CO)_2Cl_2$, eliminating the possibility that the simple electric effect by the substituents changes the product selectivity.